



*Università degli studi di Roma "La sapienza"*
*Facoltà di Ingegneria*

Tesi di Laurea Specialistica in Ingegneria delle Telecomunicazioni

*École Supérieure d'Électricité*

# Time reversal in UWB – Impulse Radio communications

**Relatore:**
Prof. Maria Gabriella Di Benedetto
**Correlatore:**
Prof. Jocelyn Fiorina

**Candidato:**
Cecchini Gabriele
matricola**:**
795279

Anno accademico 2007-2008

## Sommaire

# Chap. 1

# Preface to Time Reversal

*"Reversing time has been a compelling idea for ages. Today we can perform time reversal, leading not to the fountain of youth, but to very interesting physics and applications."*

## 1.1 Introduction

The problem of the reversibility of the time in a process can be illustrated by the following experience: a block of material explodes in many fragments and one wants creates opposite scene in order to reconstitute the block. Conceptually it is possible to consider that, after having measured the speed and the position of each one of these fragments on a sphere. One can returns then in the exact direction and with the same speed; the fragments converge then towards the initial point of explosion, as if there were film and the phenomenon pass in the

opposite direction. Indeed, the equations which control the movement of each particle are invariant by inversion of time. This experience of thought, although physically acceptable, is in reality unrealizable. Initially, the number of particles is too much large to have all information with regard them and thus to recreate the scene with back. Moreover, this chaotic system is very sensible to the initial conditions: on this type of divergent movements, an error made on an initial speed vector is propagated exponentially at the time of the reemission because of the multiple collisions between the particles. For this reason, reversal of time in traditional mechanics is impossible.

In undulating physics, on the contrary, a quantity of finished information allows to write perfectly a field of waves. Indeed the smallest detail useful for the experimenter to define the field is about the smallest wavelength contained in the system. Moreover, consequence of the linearity of the undulating system, the errors made with the emission of certain waves will not be reflected on the remainder of information as it was the case in corpuscular physic, which guarantees a quite less sensitivity to the initial conditions. For these reasons, the temporal reversal of waves is possible the same in complex systems.

## 1.2 Brief history of time reversal

Imagine the following movie: drop a pebble into a pond, and ripples propagate outward from the location where the pebble strikes the water. Now, stop the movie, and reverse it. The ripples propagate backwards and eventually converge upon the original source location reproducing the impulse due to the pebble impact that originally created the ripples, conceptually, this is Time Reversal. Meaning, Time Reversal (TR) can be thought of as a method that uses backward propagation of waves to focus wave energy onto a specific location in space and time. In 1965, Parvulescu and Clay studied what they termed a matched signal technique. In their experiment, they transmitted a signal from a source to a receiver; time reversed the received signal and broadcast it from the source to the receiver again. Parvulescu and Clay's experiment was the first demonstration of TR. This matched signal technique compensated for the coloration of the received signal due to reverberation (multi-path distortion) thereby improving the signal to noise ratio. In addition, the matched signal technique also focused the arrival of the waves in space. During the 1970s and 1980s, researchers, first in the Soviet Union, and later in the United States, created a unique mirror, called an Optical Phase Conjugator (OPC). This mirror provides the means to return an incoming wave back along the same incident ray path. Thus OPCs are similar to TR because they reverse wave energy but they differ from TR in that they function only with quasi-monochromatic waves

while TR functions with waves of any frequency bandwidth. TR was again studied in 1991 in underwater acoustics to correct the multi-path distortion and to improve the focusing of transmitted acoustic energy into a narrow beam. An important practical outcome of this work was that TR provided the means to track a moving target. Advances in microelectronics and array technologies during the beginning of the 1990s, coupled with new theoretical tools, led to the development of the acoustic Time Reversal Mirror (TRM) by Fink et al. at the University of Paris VII, Laboratoire Ondes et Acoustique (LOA); they notice that each word utter in front of an array of microphone will be listen to again but

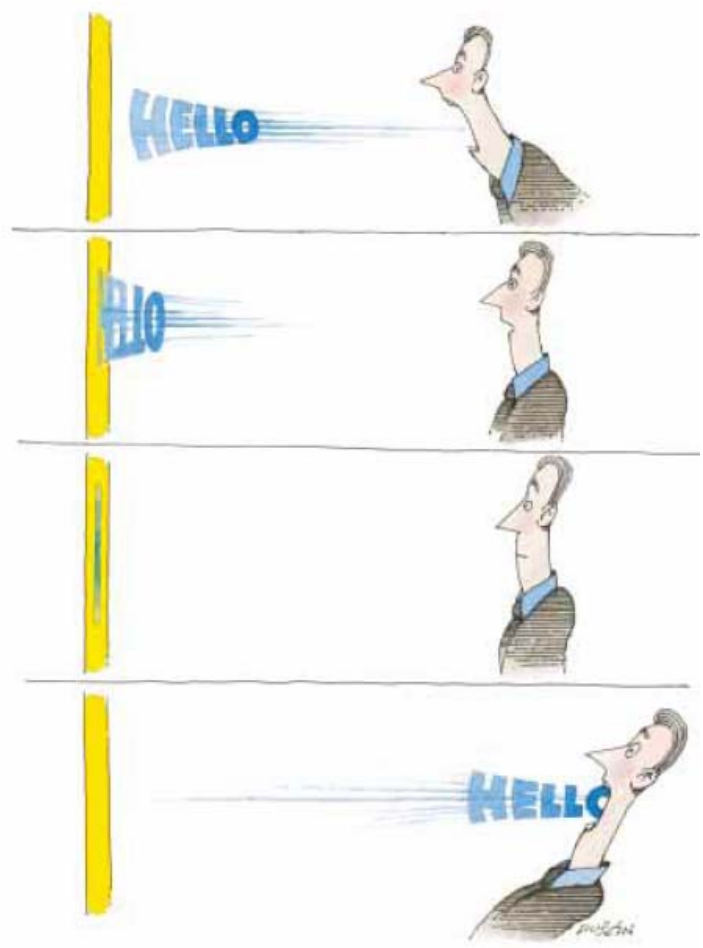


in reverse, so the echoes of the word “hello” will become ‘olleh’. The surprise was that the sound was re-broadcast exactly toward the source of the sound as the time was reversed. This process is called *acoustics time reversal* and the microphone’s array, in front of the speaker, works as *time reversal mirror*. The time reversal is possible in the acoustic because the sound is composed by wave. The vibrations produced by

the voice propagate in the air as the drop in the water. So Time Reversal process consists of a *forward propagation* step and a *backward propagation* step. In the first step, a source emits waves that travel through a medium, which are then detected by one or more receivers. The signals detected at each receiver are then reversed-in-time and rebroadcast from their respective receiver positions. The set of receivers makes up what is referred to as a TRM. The wave paths that were traversed in the forward propagation are also traversed in the backward propagation. The back-propagating waves simultaneously arrive at the original source location in phase, producing a time reversed focus, which is a reconstruction of the original source, even if reversed in time.

# Chap. 2

# Time Reversal acoustics

## 2.1 Time reversal acoustics

In acoustic the propagation of the wave in heterogeneous and non-dissipative fluid environment is governed by the following equation:

$$\rho_0(r)\nabla.\left(\frac{1}{\rho_0(r)}.\nabla\Phi(r,t)\right)=\frac{1}{c_0^2(r)}\frac{\partial^2\Phi(r,t)}{\partial t^2}$$

where $\Phi(\mathbf{r}, t)$ is the acoustical potential of the wave at the point r, $c0(\mathbf{r})$ corresponds to spatial of speed of sound of the medium and $\rho0(\mathbf{r})$ to the distribution of the density of the medium. This equation presents the property to be invariant by inversion of time. Indeed, if the potential $\Phi(\mathbf{r}, t)$ is a solution, then alike $\Phi(\mathbf{r},-t)$ is a solution because we are in the presence of derived of a even order in time. This property implies that for any wave divergent $\Phi(\mathbf{r}, t)$, there is a wave $\Phi(\mathbf{r}, -t)$ which converges towards its acoustic source. In other

words, without absorption from means during propagation, the wave equation is invariant to the transformation of time reversal. Therefore, for every burst of sound $\phi(\mathbf{r}, t)$ diverging from a source and possibly reflected, refracted or scattered by any heterogeneous media, there exists in theory a set of waves $\phi(\mathbf{r}, -t)$ that precisely retraces all of these complex paths and converges in synchrony, at the original source, as if time were going backwards.

The concept of time-reversal mirror has been developed and several devices have been built, In such a device, an acoustic source, located inside a lossless medium, radiates a brief transient pulse that propagates and is distorted by the medium. If the acoustic field can be measured on every point of a closed surface surrounding the medium (acoustic retina), and retransmitted through the medium in a time-reversed chronology, the wave will travel back to its source. Note that it requires both time reversal invariance and spatial reciprocity to reconstruct the time-reversed wave in the whole volume by means of a two dimensional time

reversal operation. From an experimental point of view a closed time-reversal mirror (TRM) consists of a two - dimensional piezoelectric transducer array that samples the wave field over a closed surface (see Figure). An array pitch of the order of $\lambda/2$ where $\lambda$ is the smallest wavelength of the pressure field is needed to insure the recording of all the information on the wave field. Each transducer is connected to its own electronic circuitry that consists of a receiving amplifier, an A/D converter, a storage memory and a programmable transmitter able to synthesize a time-reversed version of the stored signal. In practice, closed TRMs are difficult to realize and typically TRM consists of a small number of elements or time reversal channels. The major interest of TRM, compared to classical focusing devices (lenses and beam forming) is certainly the relation between the medium complexity and the size of the focal spot. A TRM acts as an antenna that uses complex environments to appear wider than it is, resulting in a refocusing quality that does not depend of the TRM aperture. The resolution is no more dependent on the mirror aperture size but it is only limited by the duration of the time reversal window and the bandwidth of the time reversed signals. It must be noticed that the research on time-reversal acoustics was initially focused

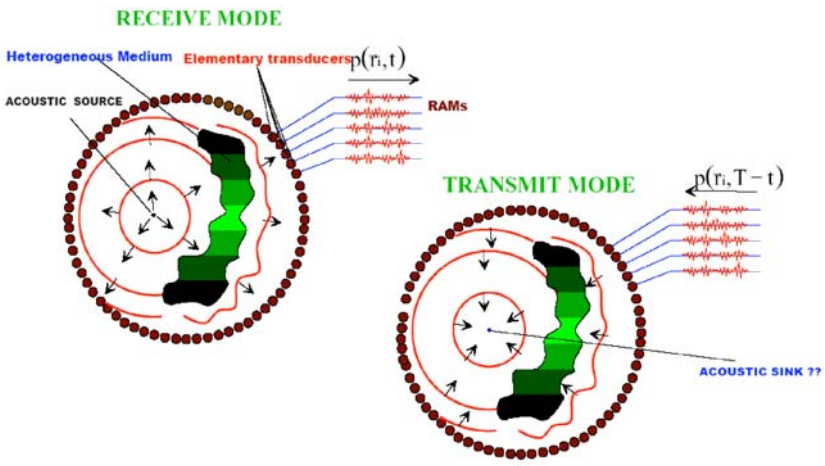

on two main applications: ultrasound therapy (tumor or kidney stone destruction) and acoustic communications in the ocean. In both applications, self focusing on the source with a TRM is accomplished without any knowledge of the medium between the source and the TRM.

## 2.2 Time reversal acoustics waveguide

When a source radiates a wave field inside a waveguide, multiple reflections along the medium boundaries can significantly increase the apparent aperture of the TRM. Thus spatial information, that is usually lost with a finite aperture TRM, is converted into the time domain and the reversal quality depends crucially on the duration of the time-reversal window (i.e., the length of the recording to be reversed). Such a concept is strongly related to a kaleidoscopic effect that appears thanks to the multiple reverberations on the waveguide boundaries, waves emitted by each transducer are multiply reflected, creating at each reflection 'virtual' transducers that can be observed from the desired focal point. A first experiment conducted in the ultrasonic regime by P. Roux et al showed clearly this effect. The time-reversal experiment is performed in the following way: (1) the point source emits a pulsed wave (1 $\mu$s duration), (2) the

TRM receives, selects a time reversal window, time-reverses and re-transmits the field which has propagated from the source through the waveguide, (3) after back propagation, the time-reversed field is scanned in the plane of the source. After the arrival of the first wave front corresponding to the direct path, we observe a set of signals, due to multiple reflections of the incident wave between the interfaces that spread over 100 $\mu$s. The figure 1b represents the signal received on one transducer of the TRM. During the re-propagation we observe a remarkable temporal compression at the source location (figure 2).

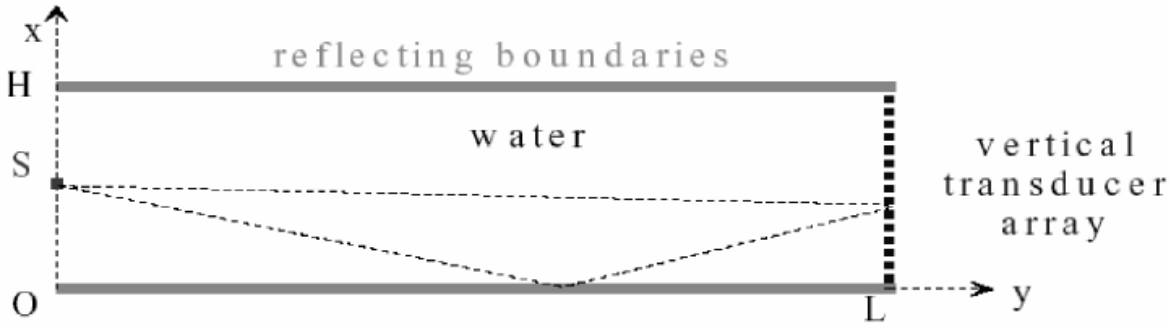

Figure 1a: schematic of the acoustic wave guide.

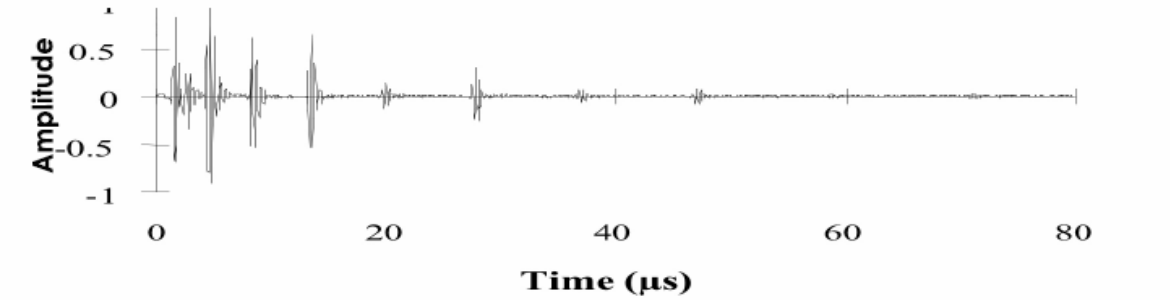

Figure 1b: temporal evolution of the signal measured on one transducer of the array

In this experiment, the transfer function of the waveguide has been completely compensated by the time-reversal process. The time-reversal process enables the compensation of the waveguide transfer function. The analysis of Figure 2

shows also that the ratio between the peak signal and the side lobe level is on the order of 45 dB.

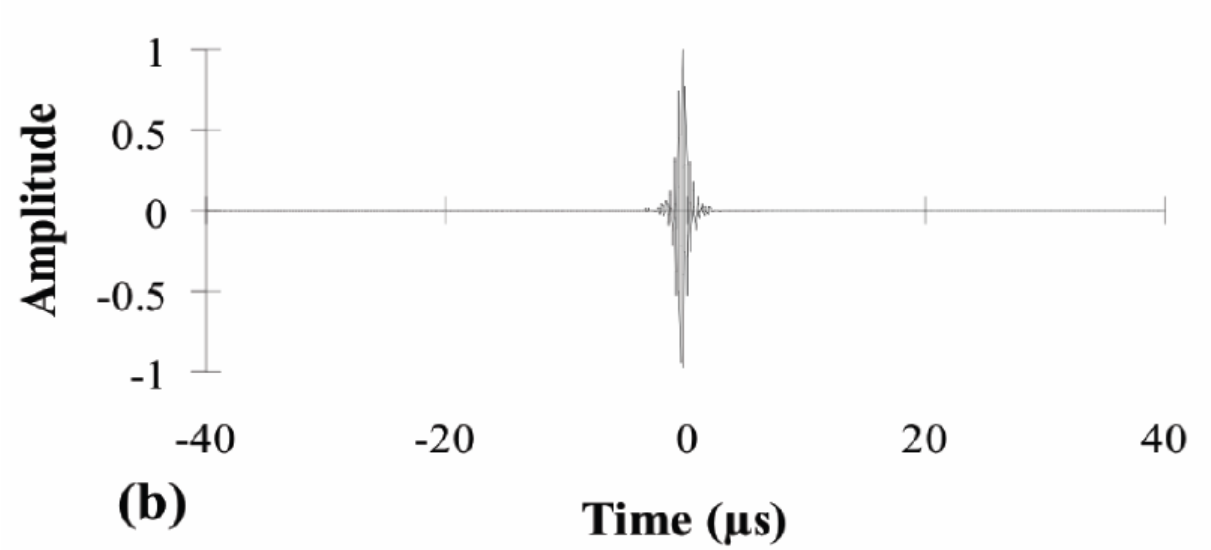


Figure 2: Time-reversed signal mesured at the point source.

Not only a remarkable time recompression is observed but the spatial focusing of the time reversed field is of interest. Figure 3 shows the directivity pattern of the time-reversed field observed in the source plane.

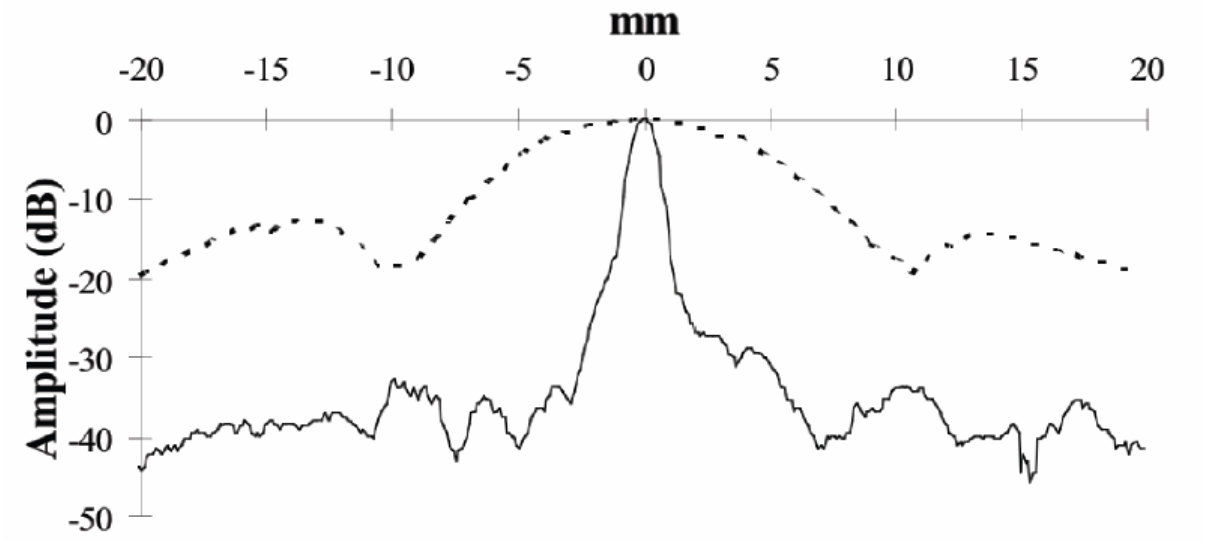


Figure 3: Directivity pattern of the time-reversed field in the plane of source: dotted line corresponds to free space, full line to the waveguide.

The time-reversed field is focused on a spot which is much smaller than the one obtained with the same TRM working in free space. For an observer, located at the source point, TRM appears to be accompanied by a set of virtual images related to multipath reverberation. The effective TRM is then a set of TRM's as shown on Figure 4.

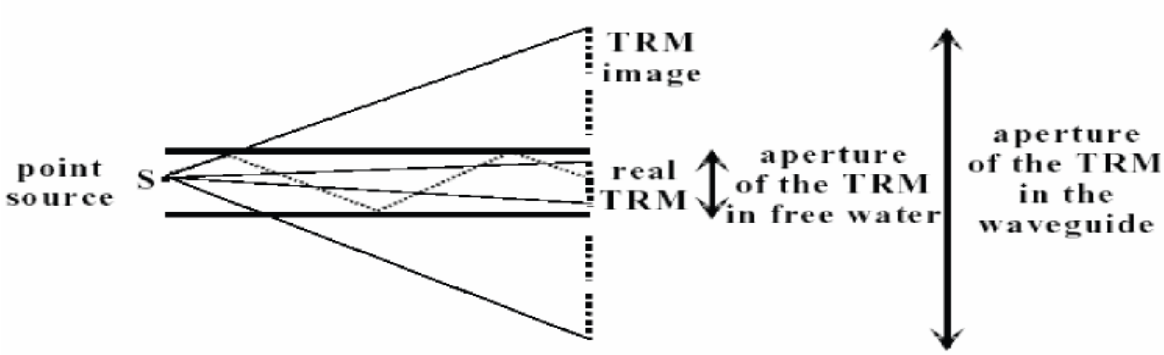


Figure 4: The principle of mirror images (Kaleidoscope) apllied to the waveguide.

Figure 5 shows the effect of the time-reversed window duration $\Delta T$ on the width of the focal spot. The size of the focal spot decreases when the number of replica selected by the window increases. This clearly shows that the effective aperture of the TRM is directly related to the time-reversal window duration $\Delta T$. Important is that the optimal time duration of the time reversal window is directly related to the waveguide dispersion and depends on the source-TRM

distance.

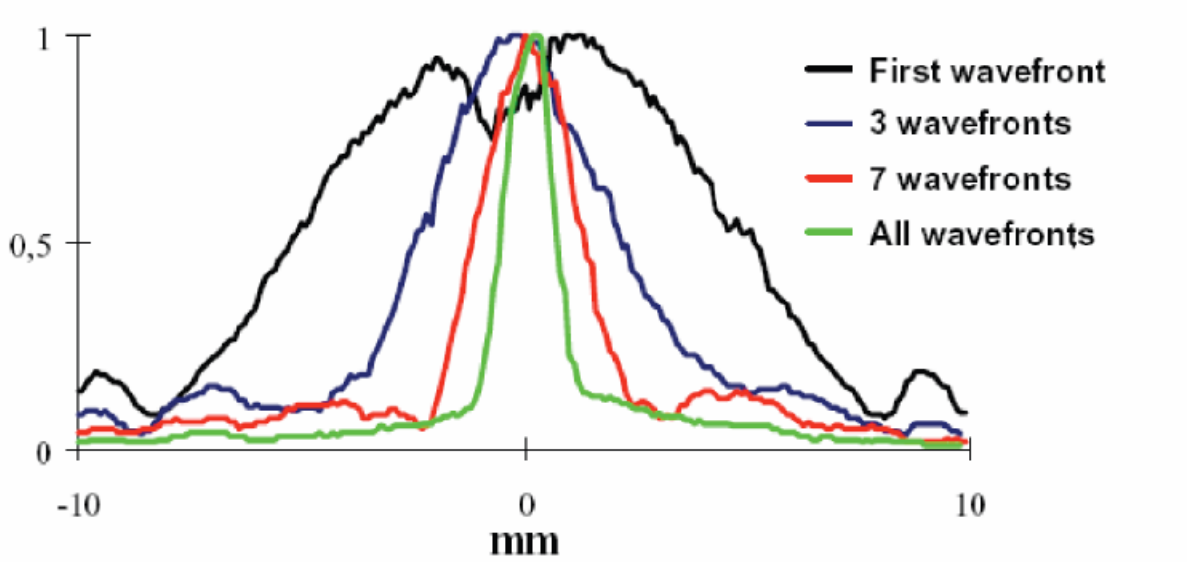


Figure 5: Directivity patterns of the time-reversal field versus the number of echoes selected in the time-reversed window

## 2.3 Time reversal: matched filter

One important aspect of this experiment is the impressive time recompression that is observed in a waveguide. It can be interpreted in terms of matched filter. We can consider that we use only monopole sources that play back the recorded pressure signals, thus the experimental time-reversed field at the source location is:

$$\varphi(r = r_0, t) \propto \sum_{i=1}^{N} G(r_0, r_i; -t) \otimes G(r_0, r_i; t)$$

It is a sum of autocorrelation functions. In terms of signal processing, wave propagation through a waveguide may be described as a linear system with

different impulse responses (Green's functions). Given a signal as input, a matched filter is a linear filter whose output is optimal in some sense. Whatever the impulse response $h_i = G(r_0, r_i; t)$, the convolution $h_i(-t) \otimes h_i(t)$ is maximum at time $t = 0$. This maximum is always positive and equals $\int h_i^2(t)dt$, i.e the energy of the signal $h_i(t)$. Indeed, with an *N*-elements array, the time-reversed signal recreated on the source depends on the sum:

$$\sum_{i=1}^{N} h_i(-t) \otimes h_i(t)$$

Even if each of the $h_i(t)$ have different behavior, each term in this sum reaches its maximum at time $t = 0$. So all contributions add constructively around $t = 0$, whereas at earlier or later times uncorrelated contributions tend to destroy one another. Thus the re-creation of a sharp peak after time-reversal on a *N*-elements array can be viewed as a process between the N outputs of *N* matched filters.

When the number *N* of channels is sufficient, that is to say when the TRM aperture fills exactly the whole waveguide aperture and when the sampling pitch is small enough, we observed that the time reversal process is not only a space-temporal matched filter but it is also a good approximation of an inverse filter of the propagation operator. However, grating lobes appear when smaller TRM are used that does not fill completely the width of the waveguide. Indeed, in this case the kaleidoscopic effect introduces a clear periodicity in the virtual array. This periodicity generates high grating lobes on each side of the main lobe. A small aperture TRM made of a reduced number of transducers does not work

perfectly, because the symmetries of the waveguide introduced grating lobes. One possibility to reduce the grating lobes is to work with broadband signals. Thus for each spectral component, the grating lobe position is shifted, so an averaging effect reduces their amplitude compared to the main lobe.

## 2.4 Time Reversal in chaotic cavities

In this paragraph we study an experiment developed in a closed reflecting cavities with no symmetrical geometry, with closed boundary conditions on information can escape from the system and a reverberant acoustic field is created. The geometry of the cavity shows ergodic properties and it means that, due the boundary geometry, any acoustic ray radiated by a point source and multiply reflected would pass every location in the cavity. Drager and Fink have showed experimentally and theoretically that in this particular case a time-reversed focusing with $\lambda/2$ spot can be obtained using only one TR channel operating in this type of cavity. The experiment is a “two step process”; in the first, one of the transducers, located at point A, transmits a short omnidirectional signal of duration 0.5μs into the water. Another transducer, located at B, observes a long chaotic signal that results from multiple reflections of the incident pulse along the boundaries of the cavity, and which continue for more than 50ms corresponding to some hundred reflections along the boundaries. At

this point, a portion ΔT of the signal is selected, time-reversed and re-emitted by point B. For time reversal windows of sufficient long duration ΔT, one observes both an impressive time recompression at point A and a refocusing of the time-reversed wave around the origin (figure 11a and 11b for ΔT=1ms). Using reflections at the boundaries, the time-reversed wave field converges towards the origin from

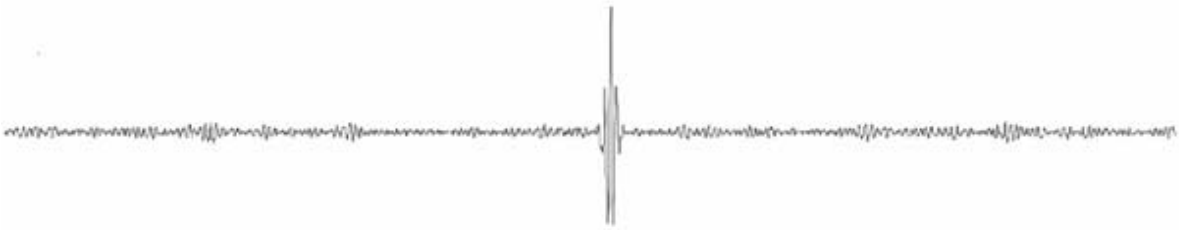

Figure 6a: Time-reversed signal observed at point A

all directions and gives a circular spot, like the one that could be obtained with a closed time reversal cavity covered with transducers. A complete study of the dependence of the spatio-temporal side lobes around the origin shows a major result: a time duration ΔT of nearly 1ms is enough to obtain a good focusing. For values of ΔT larger than 1ms, the side lobes' shape and the signal-to-noise

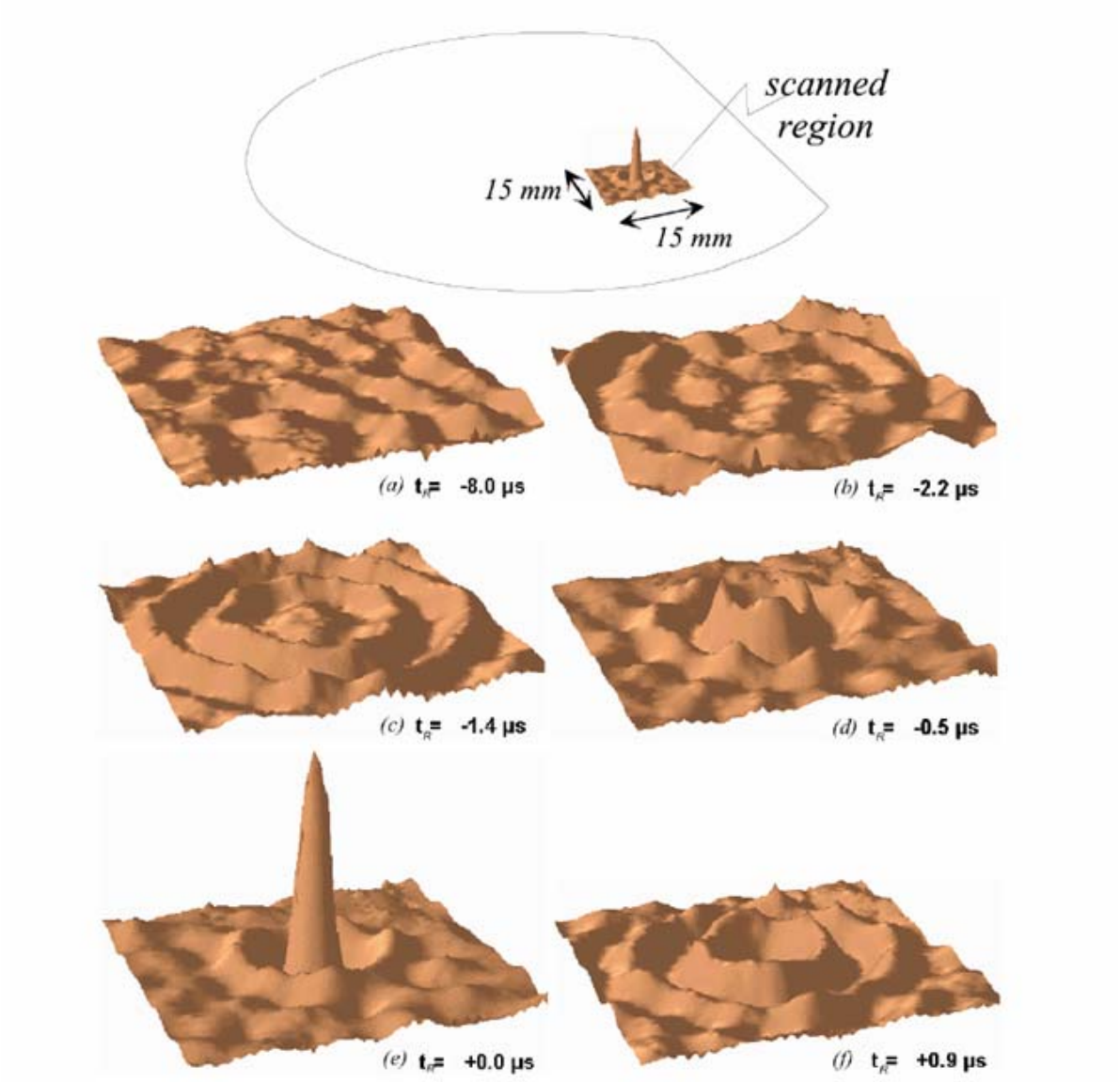


Figure 6b: Time-reversed field observed at different times around point A on a square of 15 x 15 mm2

ratio do not change any more. Once the saturation regime is reached, point B will receive redundant information on the various eigenmodes of the cavity. The saturation regime is reached after a time $T_{Heisemberg}$ that is called the Heisenberg time (in quantum chaos theory). It is the minimum time duration needed to resolve each of the eigenmodes in the cavity. It can also be interpreted as the time it takes, for all the rays radiated by a point source, to reach the vicinity of any point in the cavity in a wavelength. This guarantees enough

interference between all the multiply reflected waves to build each of the eigenmodes in the cavity. Residual temporal and spatial sidelobes persist even for time-reversal windows of duration larger than the Heisenberg time.

## 2.5 Phase Conjugation vs. Time Reversal

Optical Pase Conjugator (OPC) are similar to TR in that they reverse wave energy but they differ from TR in that they function only with quasi-monochromatic waves while TR functions with waves of any frequency bandwidth. For signal-frequency, time-reversal is equivalent to complex conjugation of amplitude. The value added of TR is the refocusing process that works only with broadband pulses, with a large number of eigenmodes in the transducer bandwidth. The averaging process that gives a good focusing is obtained by a sum over the different modes in the cavity by assuming that in a chaotic cavity we have a statistical decorrelation of the different eigenmodes, the time reversed field can be computed by adding the various frequency components (each individual mode) and it can be represented as a sum of Fresnel vectors (Figure 7). At the source position, all these phase conjugated fields have a zero phase (this comes from the phase conjugation operation that exactly compensates or the forward phase) and even if there is no amplitude focusing for each spectral contributions, there is a constructive interference

between all this fields at the focusing time as $\sum_i |H_{AB}(\omega_i)|^2$ where $H_{AB}(\omega_i)$ is the Fourier transform of $h_{AB}(t)$.

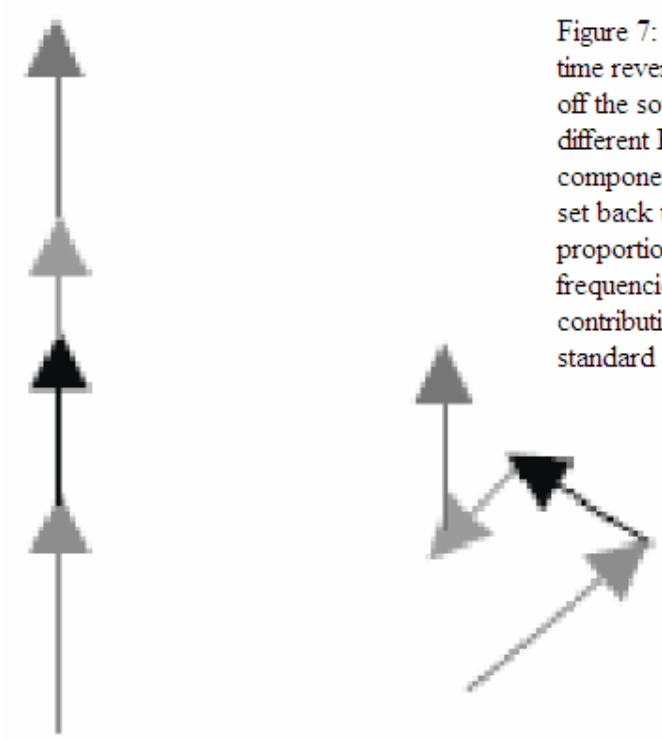

Figure 7: Schematic representation of a broad-band time reversal operation at the source (right part) and off the source (left part) . Each arrow represents a different Fresnel vector corresponding to a frequency component. At the source position, all the phases are set back to 0, the amplitude of the resulting signal rises proportionally to the number of independent frequencies N. Outside the source, the different contributions are presumably decorrelated, and the standard deviation of their sum rises as √N.

Thus, the total field at the focusing time increases proportionally to the number *I* of modes (or arrows). Outside the source position, at point **C**, we observe $\sum_i H_{AB}(\omega_i) H^*_{CB}(\omega_i)$, the contributions of each individual mode are decorrelated because there is no more coherent phase compensation and therefore the total length only increases as: $\sqrt{I}$. On the whole, the focusing peak emerges at the focusing time from the noise when the bandwidth is large enough to contain many different modes. Ideally, if we could indefinitely expand the bandwidth, the background level on the directivity patterns should decrease as $\frac{1}{\sqrt{I}}$. As the

number of eigenmodes available in the transducer bandwidth increases, the refocusing quality becomes better and the focal spot pattern becomes closed to the ideal Bessel function. As a conclusion, it must be emphasizes that in a closed cavity a one channel time reversal mirror can focused with $\frac{\lambda}{2}$ resolution if the duration of time reversal window is equivalent to the Heisenberg time of the cavity. Larger time windows do not improve the focusing quality. However, larger bandwidth $\Delta\omega$ reduces the side lobe levels as $\frac{1}{\sqrt{\Delta\omega}}$.

## 2.6 Time reversal and random medium

The ability to focus with a one channel time reversal mirror is not only limited to experiments conducted inside closed cavity. Similar results have also been

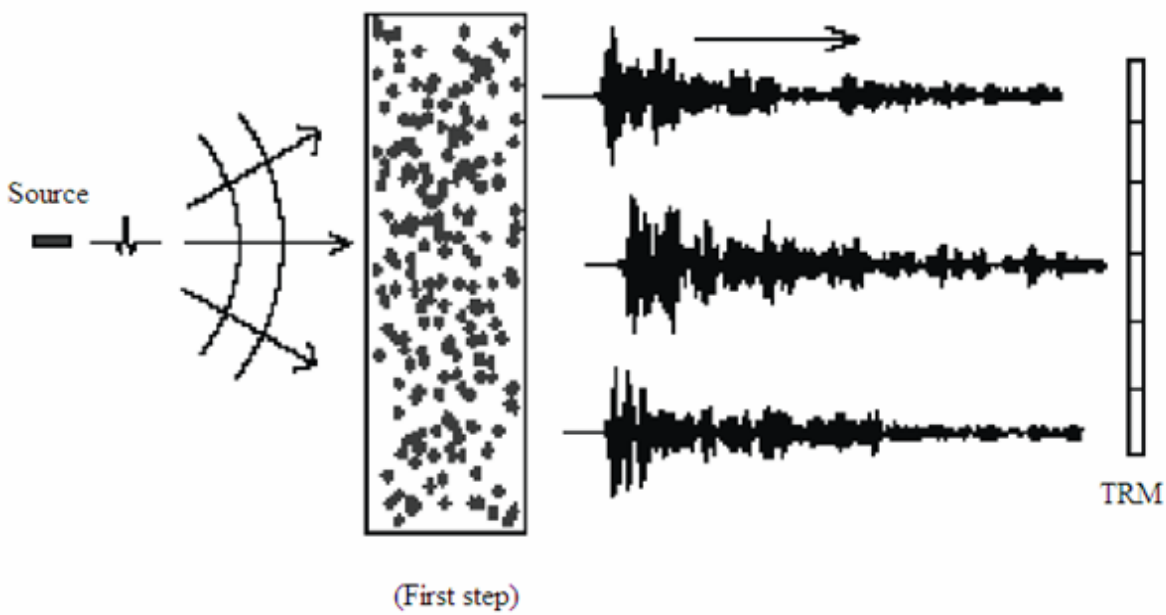


Figure 8- First step: the source transmits a short pulse that propagates through the rods and the scattered waves are recorded on a 128-element array

observed in time-reversal experiments conducted in open random medium with multiple scattering that improve the focusing quality. A. Derode carried out the first experimental demonstration of the reversibility of an acoustic wave propagating through a random collection of scatterers with strong multiple scattering contributions. A multiple scattering sample is immersed between the source and an TRM array made of 128 elements. The scattering medium consists of a set of 2000 parallel steel rods (diameter 0.8 mm) randomly distributed. The sample thickness is $L$ = 40 mm, and the average distance between rods is 2.3 mm. The elastic mean free path in this sample was found to be 4 mm (see Figure 8), The source is 30 cm away from the TRM and transmits a short (1$\mu$s) ultrasonic pulse (3 cycles of a 3.5 MHz). The figure 9 shows one part of the waveform received on the TRM by one of the element. It spread over

more than 200 $\mu$s, i.e. $\sim$200 times the initial pulse duration. After the arrival of a first wave front corresponding to the ballistic wave, a long incoherent wave is observed, which results from the multiply scattered contribution. In the second step (Figure 10) of the experiment, any number of signals (between 1 and 128) is time-reversed and transmitted and an hydrophone measures the time reversed wave around the source location.

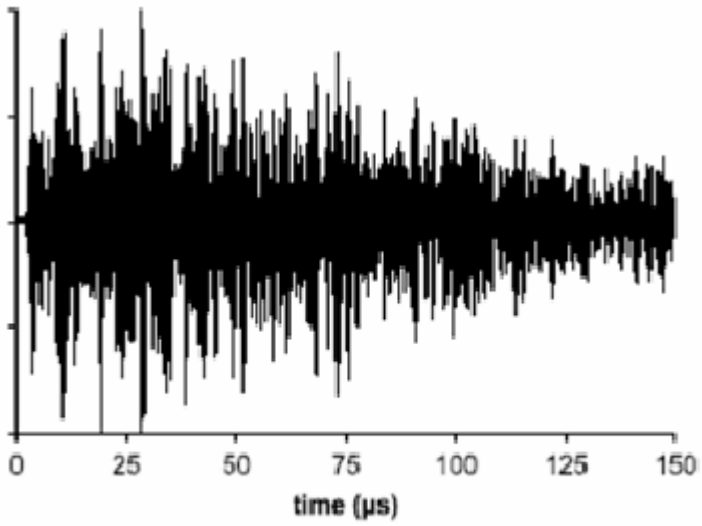

Figure 9: signal transmitted through the sample and recorded by the array element number 64

For a TRM made of 128 elements, with a time reversal window of 300 $\mu$s, the time-reversed signal received on the source is represented on Figure 11 : an impressive compression is observed, since the received signal lasts about 1 $\mu$s, against over 300 $\mu$s for the scattered signals.

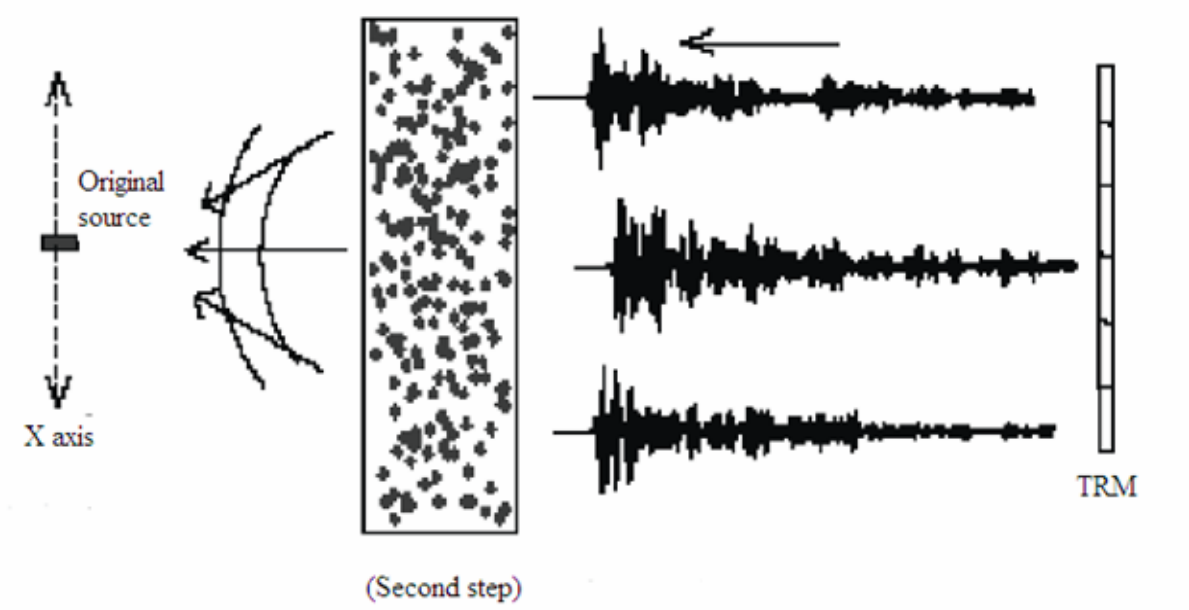


Figure 10: N elements of the array (N=1:128) retransmitt the time-reversed signals through th rods

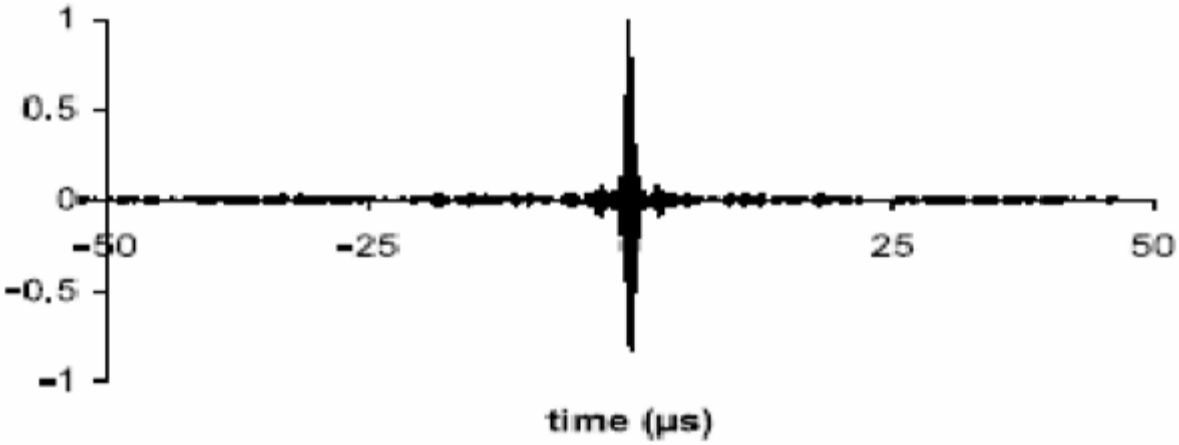


Figure 11: Signal recreated at he source after time reversal.

The directivity pattern of the TR field is also plotted in Figure. It shows that the resolution (i.e. the beam width around the source) is significantly finer than in the absence of any scattering medium: the resolution is 30 times finer, and the background level is always below −20 dB.

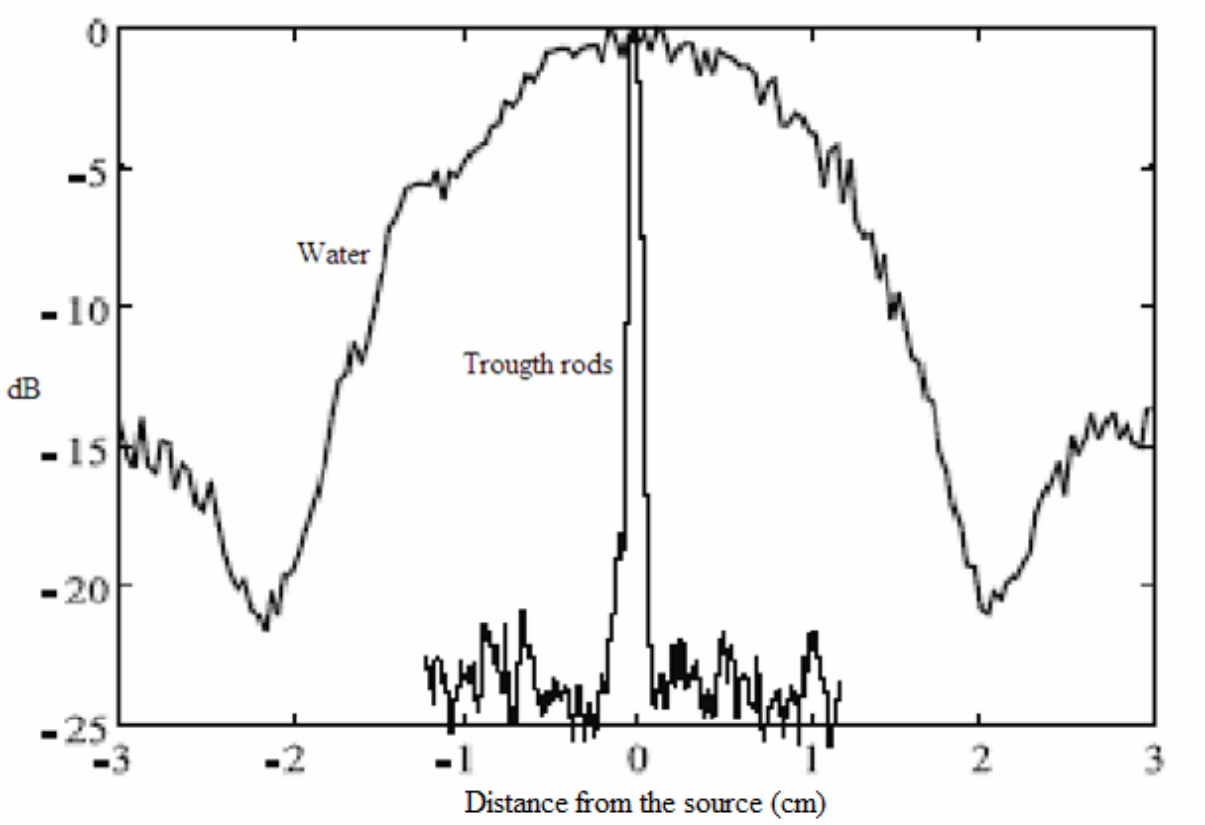


Figure 12: Directivity pattern of the time-reversed waves around the source position in the water and through the rods

We can see that high spatial frequencies that would have been lost otherwise in an homogeneous medium are redirected towards the array, due to the presence of the random scatterers distribution. Once again this result illustrates the major difference between phase conjugation and time reversal. If the experiment had been quasi-monochromatic and the array element had simply phased conjugated one frequency component, the conjugated wave field would never have focused on the source position. Indeed, whatever its phase, there is no reason for a monochromatic wave emanating from a point source to be focused on a particular point on the other side of a random sample. The phase conjugated field at one frequency in the source plane is perfectly random and verifies the

classical speckle distribution. However, if we keep in mind, that the focusing with one channel occurs only for a broadband transducer, we have to found the number of uncorrelated speckle fields that are transmitted in the transducer bandwidth $\Delta\omega$. For this, we have to define the spectral correlation length $\delta\omega$ of the scattered waves. Two monochromatic wave fields produced by a point source separated by a frequency shift of $\delta\omega$ are decorrelated. Then there are $\Delta\omega/\delta\omega$ uncorrelated spectral information in the frequency bandwidth, and the signal-to-noise is expected to depends on $\sqrt{\Delta\omega}$ . The same analysis can also be made in the time domain. Indeed, second-order moments in time and frequency are related by the Wiener-Kinchin theorem:

$$\int \langle H(\omega)H^{*}(\omega + d\omega)\rangle d\omega = \int \langle |h(t)|^2 \rangle \exp(j\delta\omega t)dt \,.$$

In other words, the spectral correlation function (averaged over the frequency bandwidth) is the Fourier transform of the 'time of flight' distribution $\langle |h(t)|^2 \rangle$ . Let $\delta t$ be the duration of the pulse obtained after time reversal (i.e. the correlation time of the transmitted signal) and $\Delta T$ the typical duration of the transmitted intensity $|h(t)|^2$. In a multiply scattering medium, in the diffusive approximation, it is known that the typical spreading time (the so called Thouless time) is equal to $T_{Thouless} = \frac{L^2}{D}$, where $D$ is a diffusion coefficient related to the mean free path. Therefore, $\Delta T$ grows proportionally to $L^2$. We have $\Delta T = 1/\delta\omega$ and $\Delta\omega = 1/\delta t$, so the number $I$ of uncorrelated frequencies grows with $L$ and may be expressed in the time or frequency domain as

$I = \Delta T/\delta t = \Delta\omega/\delta\omega \propto L2$.Instead in a dissipative medium, the time reversal process

remains a spatio-temporal matched filter, that is focused on the source, but it no more an inverse filter of the propagation. Therefore strong spatio-temporal side lobes appear. An iterative time-reversal approach must be developed to compensate for these effects.

# Chap. 3

# Time-reversal with E.M. waves

## 3.1 The first experiment

The first demonstration experiences about "Time-reversal focusing" on electromagnetic waves has been carried out from M. Fink et al. in 2004; in their experiment a source sends a short pulse that propagates through a more or less complex (but ideally non dissipative) medium and is captured by a transducer array, termed a Time Reversal Mirror (TRM). The recorded signals are

digitized, stored in electronic memories, time-reversed, re-analogized and finally transmitted back by the TRM. The time-reversed wave is structured to converge back to its source as more accurately as the medium is complex and the frequency bandwidth is larger. This is very appealing for applications in telecommunications. TRM was used to focus random series of bits simultaneously to different receivers which were only a few wavelengths apart. In the language of communication, it corresponds to a MIMO-MU configuration (Multiple Input, Multiple Output – Multiple Users). While the transmission was free of error when strong multiple scattering occurred in the propagation medium, the error rate was huge in the homogeneous medium (free space) due to crosstalk between receivers. Indeed, the spatial resolution of a TRM can be much thinner in a multiple scattering medium than in free space. In many real environments (buildings or cities), microwaves with wavelengths between 10 and 30 cm are scattered by objects such as walls, desks, cars, etc which produces a multitude of paths from the transmitter to the receiver. In such situations, a time-reversal antenna should be able not only to compensate for these multi-paths, but also increase the information transfer rate thanks to the many reflections/reverberations.

The main difficulty to transpose the time reversal technique developed for ultrasound directly to the electromagnetic case lies in the much higher sampling frequencies that are needed to digitize radiofrequency (RF) signals. Fink et al perform a truly broadband time reversal for an electromagnetic pulse

$m(t)cos(2\pi f_0 t+\varphi)$ with $f_0$ the carrier frequency and $m(t)$ a lower frequency signal ("baseband signal"). The time-reversal operation can be decomposed in two steps: phase conjugation of the wave carrier $f_0$, plus time-reversal of the baseband signal $m(t)$. The advantage is that the sampling of the baseband signal requires a sampling frequency much lower than $2 f_0$. The experiment takes place in a strongly reverberant cavity, they deliver a short pulse (central frequency 3 MHz, -6db bandwidth 2 MHz) to the 'I' analog input (Fig: 1a) of the transmit

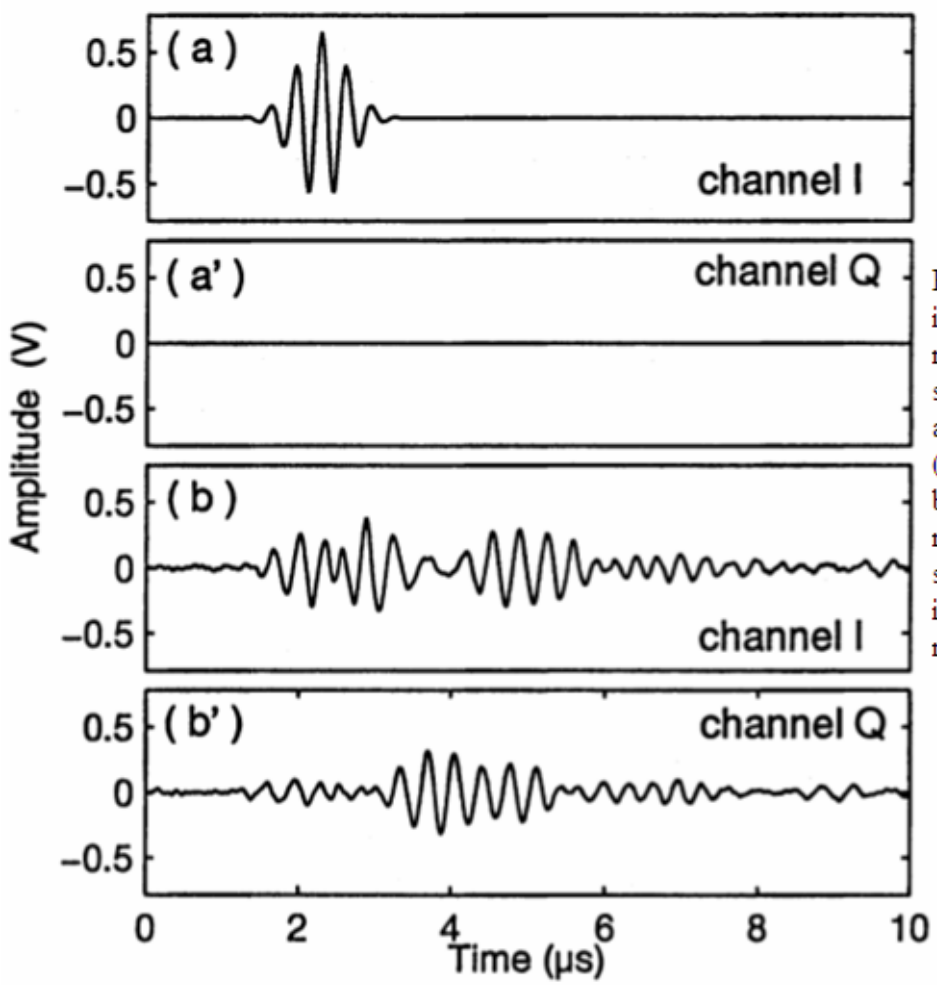


Figure 1: (a) and (a') is the baseband rappresentation of the signal transmitted by antenna A;
(b) and (b') is the baseband rappresentation of the signal reverberated inside the cavity and received by antenna B

board. No signal is delivering to the 'Q' analog input (Fig: 1a'). A mixer up converts this signal to the GHz band and delivers $e(t)=m_I(t)cos(2\pi f_0 t)$. Then the waveform $e(t)$ is transmitted by antenna $A$. After propagation, the signal

$s(t)=m'_I(t)\cos(2\pi f_0 t)+ m'_Q(t)\sin(2\pi f_0 t)$ is recorded by antenna *B* and down converted to produce the *I* and *Q* components of the output signal $m'_I(t)$ and $m'_Q(t)$ that can be observed at the oscilloscope. The signals are received last more than 8 μs, i.e. eight times longer than the initial baseband pulse or ~3200 periods of the RF. The RF wave has travelled more than two km in the 14-$m^3$ i.e. undergone ~6000 reflections. After the baseband *I* and *Q* signals $m'_I$ and $m'_Q$ are digitized by the oscilloscope at a 40-MHz sampling rate, sent to a computer and time-reversed. The wave carrier has to be conjugated too.

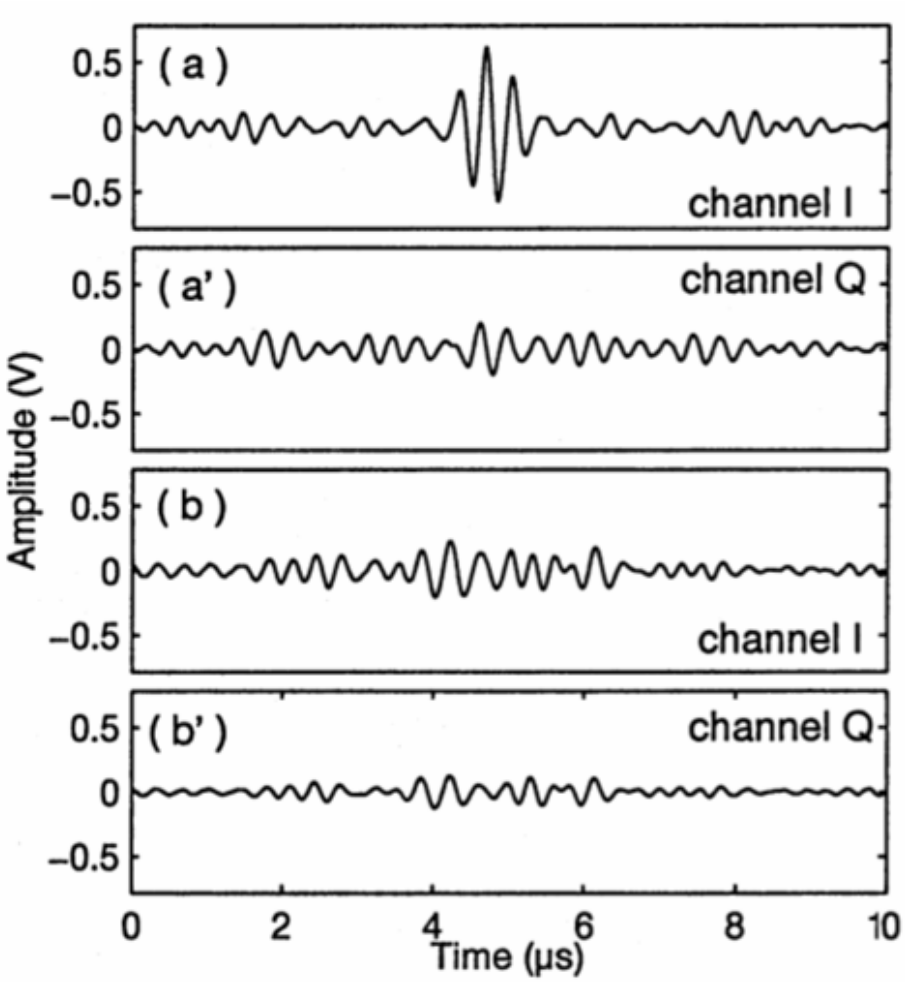


Figure 2: (a) and (a') are the baseband representation of the signal received by antenna A after time-reversal; (b) and (b') are the baseband representation of the signal received several wavelength away from antenna A after time-reversal

The following step consists in re-analogizingthe time-reversed *I* and *Q* signals, and encoding them on the phase-conjugated wave carrier; the resulting RF

signal is $m'_I(-t)\cos(2\pi f_0 t) - m'_Q(-t)\sin(2\pi f_0 t) = s(-t)$. It is then transmitted back by antenna *B*. After propagation, the RF signal received on antenna *A* is down converted to base band. As can be seen in Figure 2, the received signal on channel *I* is compressed in time and recovers its initial duration. The time reversal operation is not perfect because the reverberant wave field has been captured by a single antenna, in fact the waveform that is recreated is not the exact replica of the initial pulse: there are side lobes around the peak on channel *I*, and a signal is measured on channel *Q* (Fig. 2(a')) although nothing was sent on that channel. The peak-to-noise ratio in a one-channel time-reversal experiments varies as $\sqrt{\frac{\Delta f}{\delta f}}$ where $\Delta f$ is the available bandwidth and $\delta f$ defines the correlation frequency of the reverberated field; $\delta f$ is the characteristic width of the field-field correlation function $\int \psi(f)\psi^*(f+\delta(f))df$, with $\psi$ the scattered electromagnetic field. Therefore one could expect an even stronger pulse compression if the bandwidth was larger or the correlation frequency smaller. The experiment shows that time reversal is able to compensate for multiple reverberations and recreate a short electromagnetic pulse at the source. But there is more to it: they have also verified that the amplitude of the re-created signal is stronger at antenna *A* than anywhere else in the cavity (Fig.2 (b) and (b')). The resulting signal at the source is compressed in time and in space with a signal-to-noise ratio depending on the ratio of the bandwidth to the frequency correlation of the medium.

## 3.2 Time Reversal focusing

In a channel with rich scattering, multi paths or multiple scattering is exploited by TR to focus broadband signals tightly in space and time. The use of TR has three main benefits in communications. Temporal compression significantly shortens the effective length of the channel. For example, the complexity of a MLSE equalizer is exponential in the length of the channel; TR reduces therefore the complexity of the equalization task. Moreover spatial focusing results in very low co-channel interference in a multi-cell system. This results in a very efficient use of bandwidth in the overall system. Another advantage is the hardening of the effective channel, which means that TR results in a high diversity gain. The statistics of the time reversed channel are different from the actual channel. Specifically, the time reversed channel has a much smaller variance than the physical channel itself.

## 3.3 Temporal focusing

We can analyze the different benefits of TR for more understand its possible application in communications technology. Temporal focusing means that the channel impulse response at the receiver has a very short effective length. To characterize the amount of temporal focusing, Qiu et al have define a ratio defined as the temporal peak to total energy ratio, which characterizes the percentage energy capture by the peak of the effective CIR: $\vartheta^{TR} = E_p^{hh} / E_T^{hh}$, where $E_p^{hh}$ is the energy in the main peak of the received impulse response and $E_T^{hh}$ is the total energy in the received impulse response for the time-reversed channel. We expect this ratio to be as high as possible to illustrate good temporal compression. To illustrate temporal compression in TR, they compute the temporal peak to total energy ratio ($\vartheta^{TR}$) for LOS and NLOS at distances of 10m away from the transmitter and the results obtained are shown in the Figure 3. They have found that $\vartheta^{TR}$ is higher for the NLOS case compared to the LOS case. In fact for the LOS case reported here, $\vartheta^{TR}$ is about 59.96% while the NLOS case has a $\vartheta^{TR}$ value of about 65.73%. We can also observe some side lobes in the equivalent time-reversed channel. These side lobes are more visible for the LOS cases compared to NLOS cases. Similar results are obtained for other distances as well. This shows that temporal compression works finer for

the NLOS scenarios compared to the LOS scenario. This results show that TR is an effective way to reduce the delay spread in a UWB channel.

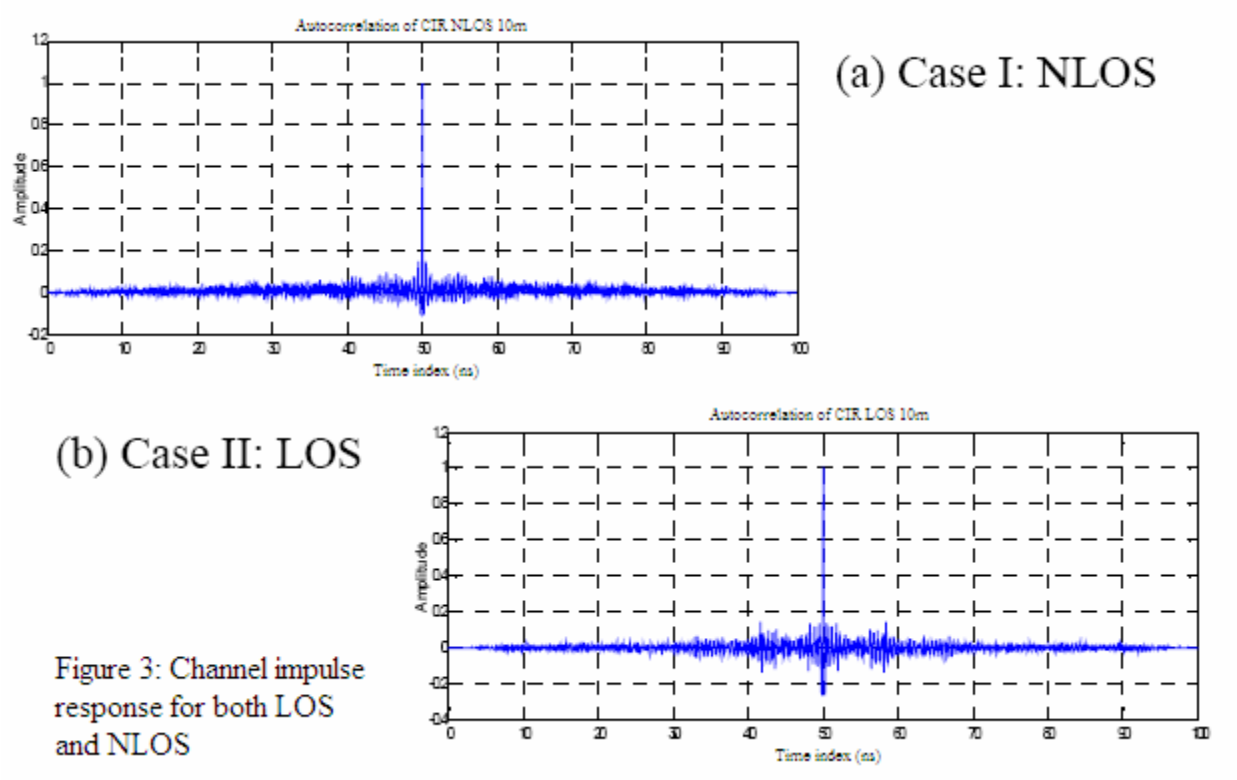


Figure 3: Channel impulse response for both LOS and NLOS

The time focusing at the focal point is described by the Root Mean Square delay spread of: $s(r,\tau) = h^*(r_0, -\tau) * h(r,\tau)$ at r = $r_0$, denoted as $\Delta\tau_0 = \Delta\tau(r_0)$. Note that this delay-spread is defined as:

$$\Delta\tau(r) = \sqrt{\frac{\int(\tau - \tau_m)^2 |s(r,\tau)|^2 d\tau}{\int|s(r,\tau)|^2 d\tau}}$$

where $\tau_m$ is the average delay defined as:

$$\tau_m(r) = \frac{\int \tau\, |s(r,\tau)|^2\, d\tau}{\int|s(r,\tau)|^2 d\tau}$$

and accounts for the pulse width. Finally, a time focusing gain (TFG) is also suitably defined by the relative increase of RMS delay spread $\Delta\tau(r)$ at any point r compared to $r_0$. The parameter is defined as: $\sigma(r) = \frac{\Delta\tau(r) - \Delta\tau_0}{\Delta\tau_0}$.

A larger TFG indicates better temporal focusing in the sense that the time compression at the focal point with respect to any point away from the focal point becomes larger.

## 3.4 Spatial focusing

The second advantage of TR we said that is: Spatial focusing. Spatial focusing means that the spatial profile of the power peaks at the intended receiver and decays rapidly away from the receiver. S. M. Emani et al. have studied the remarkable space focusing properties of signal transmission with time reversal. In order to study the effects of TR they measure the channel impulse response between the transmitter and a receiver. They repeat the measurement by holding the transmitter fixed and changing the position of the receiver over a square grid. They take one corner of the grid as the reference receiver (the intended receiver) and use its impulse response as the transmitted prefilter $h^*(r_0, -\tau)$. The time reversed field at any point on the square grid can now be computed based on the channel measurements and by using the following equation:

$$s(r,\tau) = h^*(r_0, -\tau) * h(r,\tau)$$

where * denotes convolution with respect to delay. This is equivalent to having the transmitter that performs the pre-filtering with the TR filter to send at the receiver on r0. The power of the signal as a function of both space and delay is computed and investigated. As a metric for spatial focusing they define the following quantity:

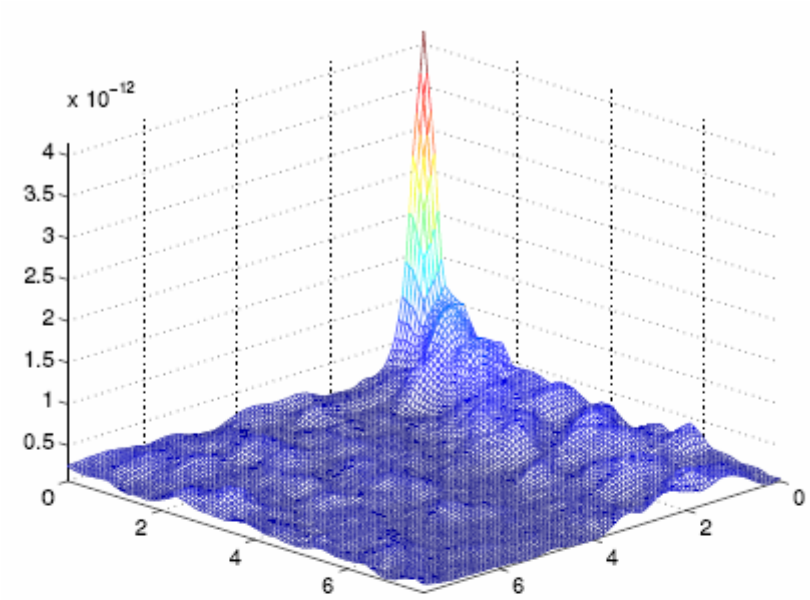


(a) Case I

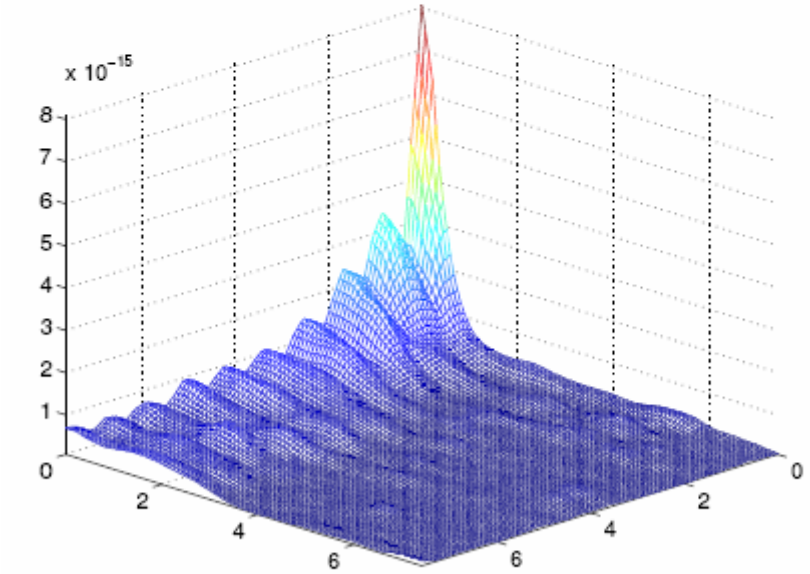


(b) Case II

Figure 4: Spatial focusing κ(r). One shot spatial field realizations for a), the line-of-sigth and b) the non-ligth-of-sigth scenario

$$\kappa(r) \triangleq \max_{\tau} |s(r,\tau)|^2$$

this quantity represents the power of the strongest tap at a receiver located at r. We expect $\kappa(r)$ to peak at $r_0$ and to decay rapidly with increasing distance from the origin. The environment is an office space (40m x 60m) with many cubicles. Measurements span the bandwidth 2-8 GHz with 3.75 MHz

frequency resolution. From the data we estimate that the coherence bandwidth of the channel is 20 MHz. The virtual grid on which the receiver is moved has a distance of $\frac{\lambda_0}{4}$ where $\lambda_0$ is the wave length of the mid frequency of the measurements (5 GHz). The receiver antenna is moved to a different location with a precise robotic positioner. They evaluated two different scenarios: *Case I* is a line-of-sight scenario with a separation of 3m; *Case II* has a separation of 11m and is a non-line-of-sight situation. In the 3-D figures, the square grid spans a region of $7\lambda_0$ x $7\lambda_0$. A 3d plot of $\kappa(r)$ of the two cases is shown in Figure 4. We see that spatial focusing works fine in both scenarios and we also observe that the signal power level is at least 10dB lower at a distance of $7\lambda_0$ than its value at the receiver. This demonstrates the spatial decorrelation very well. We can conclude that channel impulse responses show inherent quasi-orthogonally in space, which can be used for interference suppression. Also the spatial focusing means that there is a very low probability of intercept by a neraby receriver.

## 3.5 Diversity gain

When a short pulse propagates through a complex medium, scattering or reverberation spreads the initial pulse over a characteristic time $\tau$. If the scattered signal is time-reversed through the same reciprocal medium, it can been shown that the amplitude of the refocused pulse is proportional to $\tau\Delta\nu$

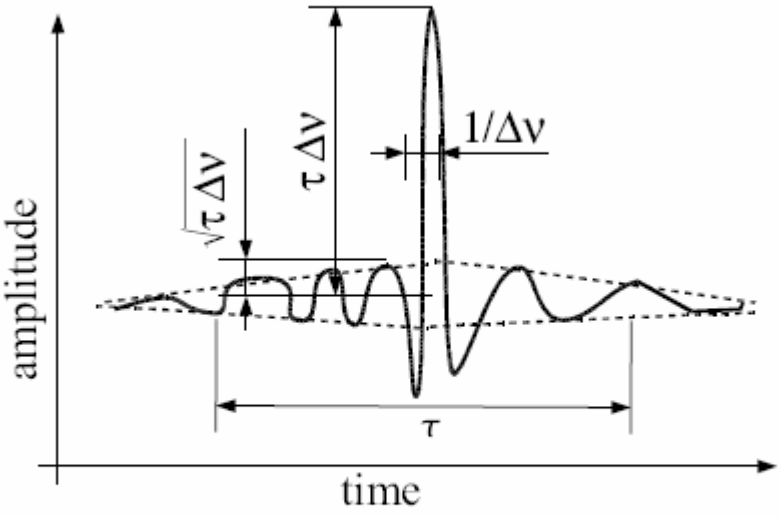


Figure 5: Schematic representation of the time compression after TR of a scattered wave issued from a single pulse. The amplitude of the pulse is proportional to τΔν. the decay time of the sidelobes is ≈τ and their typical height is √τΔν

($\Delta\nu$ the bandwitth of the initialy emitted pulse) while the standard deviation of the sidelobes surrounding the peak is proportional to $\sqrt{\tau\Delta\nu}$.

Figure 5 showes the schematic representation of the time compression after TR of a scattered wave issued from a single pulse. The amplitude of the pulse is proportional to $\tau\Delta\nu$. The decay time of the sidelobes is $\approx \tau$ and their typical height is $\sqrt{\tau\Delta\nu}$. This study subscrib that a great wide band signal is a perfect actor to use time reversal techinique:Infact the wide band improves the gain of diversity and all the aspects connected as temporal focusin and spatial focusing.

## 3.6 Time reversal and its applications

AllTR's advantages that we have saw us the possibility to discover new commuincation system which the goal is to improve the quality and the optimazation of the communications. A perfect actors for time reversal are the

UWB signals. The UWB channel impulse response (CIR) contains a large number of resolvable components coming from different paths, in particular in indoor environments. We can use time reversal as a signal focusing technique that turns multipath and all the limits of a traditional communications (and even Inter Symbol Interference) into a benefit. The idea is to use the channel impulse response as a pre-filtering. Therefore in a UWB-TR communication the time reversed channel impulse response (CIR) of any transmit-receive link is taken as a prefilter at the transmitter. If such a time reversed sequence is irradiated into the channel, its components retrace their former paths and lead to a focus of power at the intended receiver at some particular time instant. The goals of ambitious project is to combine and to reduce the complexity of the receiver, to make the communications more robust in the presence of narrowband interference relative to receiver-equalization-based UWB and to reduce the co-channel interference in a multi-user system too. This technique has also drawbacks and limits in particular: the channel must be reciprocal to allow an easier time reversion, the channel must be stable in time during the propagation of the signal pre-filtered and we must valuate the possibility of channel correlation between users.

# Chap. 4

# Time-reversal with UWB-IR signal

## 4.1 UWB introduction

The world of ultra-wideband (UWB) has changed dramatically in very recent history and in particular a substantial change occurred in February 2002, when the Federal Communications Commission (FCC) issued a ruling that UWB could be used for data communications as well as for radar and safety applications. The band that the FCC allocated to communications is 7.5 GHz between 3.1 and 10.6 GHz; by far the largest allocation of bandwidth to any commercial terrestrial system. The first definition for UWB comes from the

Defense Advanced Research Projects Agency (DARPA) and it provides that a signal, can be classified as an UWB signal if $B_f$ is greater than 0.25. The fractional bandwidth can be determined as: $B_f = 2\frac{f_h - f_l}{f_h + f_l}$ where $f_l$ is the lower and $f_h$ is the higher -3 dB point in a spectrum, respectively. In February 2002 the prevailing definition has decreased the limit of $B_f$ at the minimum of 0.20, defined using the equation above. A signal with an energy bandwidth of 2 MHz, for example, is UWB if the center frequency of its spectrum is lower than 10 MHz, note that the definition of an UWB signal can give only relatively to the center frequency. The FCC has also defined that $f_l$ and $f_h$ are set to the lower and upper frequencies of the -10dB emissions points. The possibly for UWB in communication are a lot. First, the enormous bandwidth of the system meant that UWB could potentially offer data rates of the order of Gbps. Second, the bandwidth was overlaid on many existing allocations and due to the low energy density and the pseudo-random characteristics of the transmitted signal, the UWB signal is “noiselike”, which makes unintended detection quite difficult. Third, the very narrow time domain pulses mean that UWB radios are potentially able to offer timing precision much better then GPS.

## 4.2 Impulse Radio UWB

The most common and traditional way of emitting an UWB signal is by radiating pulses that are very short in time and “very short “ refers to a duration of the pulse that is typically about few hundred picoseconds. This transmission technique goes under the name of Impulse Radio and has the significant advantage of being essentially a baseband technique. Therefore this aspect reduces the complexity and the cost of UWB systems. Unlike conventional radio systems, the UWB transmitter produces a very short time domain pulse, which is able to propagate without the need for an additional RF (radio frequency) mixing stage. The RF mixing stage takes a baseband signal and ‘injects’ a carrier frequency or translates the signal to a frequency which has desirable propagation characteristics. The very wideband nature of the UWB signal means it spans frequencies commonly used as carrier frequencies. The signal will propagate well without the need for additional up-conversion and amplification. The reverse process of down-conversion is also not required in the UWB receiver. Again, this means the omission of a local oscillator in the receiver, and the removal of associated complex delay and phase tracking loops. The way by which the information data symbols modulate the pulses may vary: Pulse Position Modulation (PPM) and Pulse Amplitude Modulation (PAM) are commonly adopted modulation schemes. In addition to modulation and in order

to shape the spectrum of the generated signal, the data symbols are encoded using pseudorandom or pseudo-noise (PN) codes.

## 4.3 Pulse Amplitude Modulation

The classic binary pulse amplitude modulation (PAM) can be presented using e.g. two antipodal Gaussian pulses as shown in Figure 1. The transmitted binary baseband pulse amplitude modulated information signal (t) can be presented as:

$$x(t) = d_j \cdot w_{tr}(t)$$

where $w_{tr}(t)$ represents the UBW pulse waveform, j represents the bit transmitted (‘0’ or ‘1’) and :

$$d_j = \begin{cases} -1, j = 0 \\ 1, j = 1 \end{cases}$$

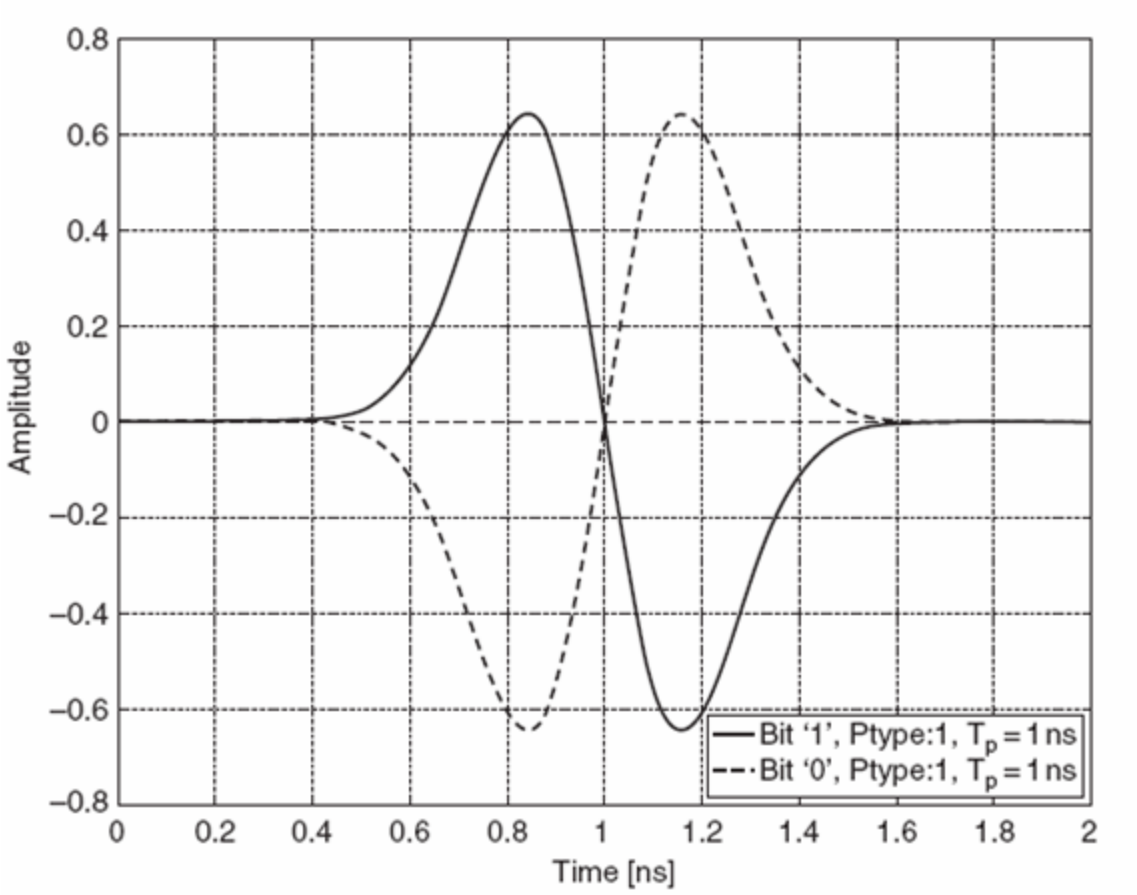


Figure 1: BPAM pulse shapes for '1' and '0' bits

There are also many different modulation schemes that may be used with UWB system, as pulse position modulation (PPM) or on-off keying (OOK) or pulse shape modulation (PSM) but we have decided to apply only PAM modulation scheme to UWB with Time Reversal and for other modulation scheme refer to appropriated book.

## 4.4 UWB receivers

UWB systems can be characterized by a bandwidth extension as traditional spread spectrum (SS) systems but one of the major differences between UWB

systems and traditional SS systems is the radio channel which they use; the UWB channel is extremely multipath rich. If we combine the different paths we can increase the total signal power otherwise if the multipath components are not combined they lead to interference. The significantly greater number of resolvable multipath components associated with UWB system's much greater bandwidth means that many more receiver elements need to be considered. The received signal energy can be improved in a multipath fading channel by utilizing a diversity technique, such as the rake receiver (Proakis, 1995). Rake receivers combine different signal components that have propagated through the channel by different paths. The optimum correlator for the present case must include additional correlators associated with different replicas of the same transmitted waveform. The Rake receiver consists of a parallel bank of $N_r$ correlators, followed by a combiner that determines the variable to be used for the detection on the transmitted symbol. Each correlator is locked on one of the different replicas of the transmitted symbol. This can be characterized as a type of time diversity. The combination of different signal components will increase the signal-to-noise ratio (SNR), which will improve link performance. More the rake receiver there are also different receivers that we can utilize as Minimum Mean Square Error (MMSE) or an easier energy detector. As usual we select the best for our application.

## 4.5 Rake Receiver Types

The adoption of Rake considerably improve the complexity of the receiver and this complexity increase with the number of multi-path components analyzed and combined before decision. The ideal rake receiver structure captures all of the received signal power by having a number of fingers equal to the number of multipath components. The so called ideal-rake or all-rake (I-rake and A-rake) is such a receiver. The problem with this approach is the need for an infinite number of rake branches, which also means an infinite number of correlators. Consequently, implementation of the A-rake is not possible in reality. All of the paths that arrive within the receiver's time resolution will be seen as a single path. The energy of the single path is a combination of the energy of all of the undistinguishable paths. A practical rake receiver implementation is a selective rake, called S-rake. The S-rake only uses the $L_r$ strongest propagation paths. Therefore information on the channel impulse response is required in order to use the S-rake. Channel estimation algorithms must be used to obtain this a-priori information. The SNR is maximized when the strongest paths are detected. The link performance will be improved relative to the single path receiver. The complexity of the S-rake receiver is greatly reduced relative to the A-rake by only selecting those multipath components that have significant magnitude. Depending on the channel delay profile, the selected paths can be consecutive, or spread over the profile. The partial-rake receiver, P-rake, is a

simplified approximation to the S-rake. The P-rake involves combining the Lr first propagation paths. The principle behind this approach is that the first multipath components will typically be the strongest and contain the most of the received signal power. The disadvantage is that the multipath components that the P-rake receiver combines are not necessarily the strongest multipath components, so optimum performance will not be achieved. Under ideal conditions, the A-rake outperforms the S-rake, which typically outperforms the P-rake. However, if the strongest propagation paths are at the beginning of the channel impulse response, the S-rake and P-rake will give the same performance.

## 4.6 MMSE Receiver

For high data rate UWB system in the presence of Inter Symbol Interference (ISI) and Multi Access Interference (MAI), an MMSE multiuser detection receiver outperforms a conventional Rake receiver.

## 4.7 Energy detector receiver

Practical and low complexity implementation of receivers is of vital importance for the successful penetration of the ultra wideband (UWB) technology. Energy detector receiver is an attractive solution for UWB signal reception trading off complexity with performance. The energy detectors is achieved by passing the signal through a square law device followed by an integrator and a decision

mechanism, where the decisions are made by comparing the outputs of the integrator with a threshold. Two challenging issues for the enhancement of energy detector receivers are the estimation of the optimal threshold, and the determination of synchronization/dump points of the integrator. The optimal threshold in an energy detector receiver depends on the noise variance, multipath delay profile, received signal energy, integration interval, synchronization point, and the bandwidth of the band pass filter. Moreover the optimal interval, which minimizes the BER, can ideally be achieved by a joint and adaptive determination of the starting point and duration of integration. Let the impulse radio (IR) based UWB signal received for bit *i* in a multipath environment be represented as:

$$r_i(t) = \sum_{j=1}^{N_s} \left(s_j(t) + n_j(t)\right),$$

where we have:

$$s_j - \sum_{l=1}^{L} \gamma_L b_i \omega_l \left(t - jT_f - c_j T_C - \tau_l\right),$$

the number of pulses per symbol is denoted by $N_s$, L is the number of multipath components arriving at the receiver, *j* and *l* are the frame and tap indices, respectively, $b_j$ is the *j*-th transmitted bit with PAM modulation, $\omega_l(t)$ is the received pulse shape for the *l*-th path, $T_f$ is the frame duration ( $T_f > \tau_L > T_c$ ), $c_j$ are the time-hopping codes, $\gamma_l$ and $\tau_l$ are the fading coefficient and the delay of the *l*-th multipath component, respectively and $T_C$ is the chip duration.

The additive with Gaussian noise (AWGN) with double-sided noise spectral density $\frac{N_0}{2}$ is denoted by $n_j(t)$. The received signal is passed through a band pass filter of bandwidth B to capture the significant portion of signal spectrum while removing out-of-band noise and interference. Now consider an energy detector, where the following decision statistic is used to make symbol detection by sensing the energy level within the symbol interval:

$$h_i = \sum_{j=1}^{N_s} \int_{T_i} \left[ \sum_{l=1}^{L} \gamma_L b_i \omega_l \left( t - jT_f - c_j T_c - \tau_l \right) + n_j(t) \right]^2 dt$$

Where $T_i$ is the integration window defined by synchronization and dump point. In other words the above approach for the energy detector integrates the square of the received signal for each pulse position over the maximum excess delay of the channel and sums these statistics over $N_s$ pulses. The symbol decision is performed by comparing $h_i$ with a threshold $\xi$, $h_i \lessgtr \xi$.

## 4.8 UWB signal synchronization

The receiver must, in general, extract discrete time information from the received continuous waveform to reconstruct at best the discrete sequence of symbols emitted by the source; precise information about frequency and phase of the emitted symbols, after distortion by the channel, must be either available

or recovered at the receiver. Due to the very short duration of the transmitted pulses, receiver performance is in fact very sensitive to synchronization errors. Different algorithms for UWB signal acquisition have recently been proposed. In a synchronization scheme the accounts for the way information is typically structured into packets by the MAC module is introduced. The proposed algorithm is based on the presence of a fixed synchronization trailer at the beginning of each packet, and assumes that synchronization can be maintained for the entire duration of a packet. For each single packet, synchronization must be re-established. This scheme accounts for the presence of clock drifts between the two stations involved in the synchronization process; within a packet, the procedure keeps track of synchronization, while in between two packets, when tracking is not active, synchronization might be lost after a time lag that depends on time drifts of local oscillators. Each data packet generated by the UWB transmitter is composed of three parts: trailer synchronization, a header that contains control information plus signaling symbols for channel estimation and error detection, and a payload for the user data. The synchronization trailer consists of a sequence of M pulses and is known *a priori* by all network participants. The trailer allows a receiver to detect incoming packets. Correlation filters that are matched to the synchronization trailer are in fact implemented in all receiving stations. Synchronization performance is directly related to the M value. Estimated M values fall in the range of 40-100 pulses for a wide range of applications.

## 4.9 UWB and Time Reversal

Different studies have proposed that the application of time reversal to UWB will give many advantages at the communications. The most important aspect is the possibility to reduce the receiver complexity, as we have see using the channel impulse response time reversed as a pre-filter we obtain a focalization but a compression too. This aspect can improve the low cost aspect that should give at UWB system an ulterior push to become a reality. The real advantages of this joint are the possibility to use a non-coherent detection for extremely low cost.